

The exclusive license for this PDF is limited to personal printing only. No part of this digital document may be reproduced, stored in a retrieval system or transmitted commercially in any form or by any means. The publisher has taken reasonable care in the preparation of this digital document, but makes no expressed or implied warranty of any kind and assumes no responsibility for any errors or omissions. No liability is assumed for incidental or consequential damages in connection with or arising out of information contained herein. This digital document is sold with the clear understanding that the publisher is not engaged in rendering legal, medical or any other professional services.

Chapter 5

LASER INTERFERENCE LITHOGRAPHY

Henk van Wolferen and Leon Abelmann

MESA+ Research Institute for Nanotechnology,
University of Twente, Enschede, The Netherlands

ABSTRACT

In this chapter we explain how submicron gratings can be prepared by Laser Interference Lithography (LIL). In this maskless lithography technique, the standing wave pattern that exists at the intersection of two coherent laser beams is used to expose a photosensitive layer. We show how to build the basic setup, with special attention for the optical aspects. The pros and cons of different types of resist as well as the limitations and errors of the setup are discussed. The bottleneck in Laser Interference Lithography is the presence of internal reflection in the photo-resist layer. These reflections can be reduced by the use of antireflection coatings. However the thicknesses of these coatings depends on the angle of exposure and the material property or combination of materials in thin films. We show with some examples how to deal with this issue. Finally we show examples of more complex patterns that can be realized by multiple exposures.

1. INTRODUCTION

In 1801 Thomas Young established the wave theory of light by means of his famous double slit experiment. This experiment showed the effect of the interference of light in beautiful colors.

Humphrey Lloyd describes in 1843 the use of a mirror to show interference of light.

In 1891 Nobel Prize winner Gabriel Lippmann used interference of light to create the first color photograph. For this he used a glass plate with a fine grain high-resolution photosensitive layer (Lippmann-emulsion film) in contact with a high reflecting (mercury) surface as a mirror.

Dennis Gabor published the first hologram in 1948 as “A New Microscopic Principle” based on interference. In 1960 Theodore H. Maiman demonstrated the first functioning laser

at Hughes Research Laboratories. This was the start of using interference as a useful tool to measure distances, speed and accelerations but also to create holograms as shown by Emmett Leith at the Optical Society's 1964 Spring Conference. The laser found its way into more and more applications.

In 1967 P.H. Langenbeck[4] used a laser as a source for the Lloyd's interferometer for flatness testing over a large surface. Around 1970 several researchers were experimenting with photoresist to create holograms and diffraction gratings, and holographic or Laser Interference Lithography was born. Ever since, the Lloyd's Mirror Interferometer has been used to either push the limits of lithography or to create a simple setup to create high-resolution line patterns on almost any surface structure. The depth of focus is unique in the world of lithography. Not just a few microns but millimeters or even meters are possible in Laser Interference Lithography. There are also disadvantages like the difficulty in aligning it to another structure.

In the last 40 years the Lloyds' Mirror Interferometer has been used as a lithography tool for many applications. It started as a flexible tool to use to make gratings for coupling into optical waveguides. The double exposure at 90° and 60° found its application in magnetic recording[6], micro sieves[8] and 2D-photonics crystals[9].

2. THEORY

When two laser beams from the same source coincide, an interference pattern is created as illustrated in figure 1. Their intensity and phase relation result in a holographic pattern consisting of dark and bright spots containing all information about the two interfering beams.

The intensity I_r of this spot can be described by

$$I_r = I_1 + I_2 + 2\sqrt{I_1 I_2} \times \cos \varphi \quad \text{Equation 1.[1]}$$

where φ is the phase difference between the two beams at that particular place. The phase difference φ is due to the angle between the two coherent laser beams. The two laser beams will only interfere over a distance where their phase-relation is constant. This distance is called coherence length and depends on the bandwidth of the laser. If the wave-front of the laser is free of any distortion, we obtain structures of lines with a well-defined spacing: a diffraction- or Bragg-grating.

The period of this periodical structure Λ is

$$\Lambda = \frac{\lambda}{\sin(\theta_1) + \sin(\theta_2)} \quad \text{Equation 2.}$$

where λ is the wavelength of the laser and angle θ_1 and angle θ_2 are the angles between the normal of the exposed surface and the beams 1 and 2, as is indicated in figure 1. The intensity of the grating is sinusoidal and can be used for different applications. In the following we will discuss the lithographic ability of this sinusoidal interference pattern by exposing it to a photosensitive layer, either positive or negative.

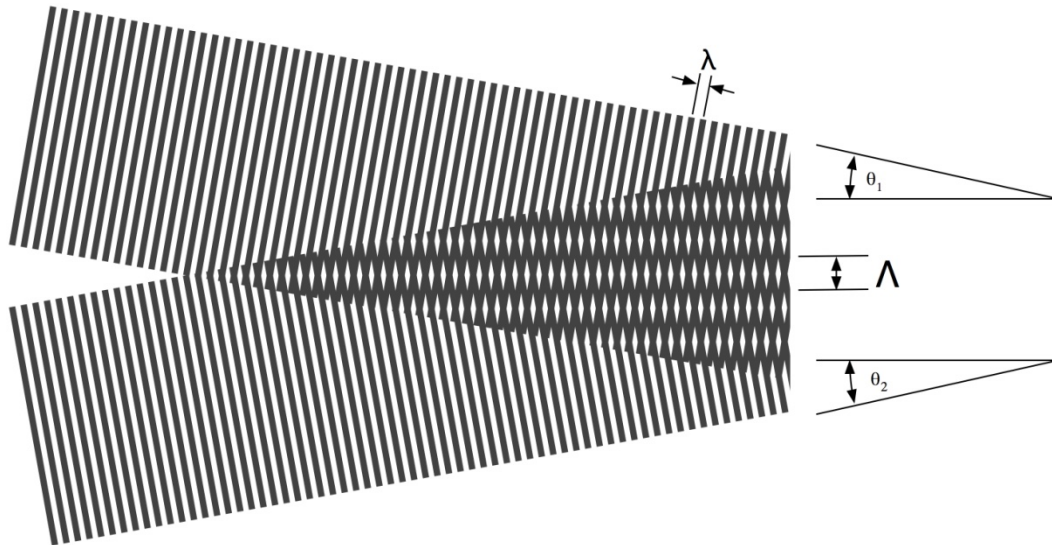


Figure 1. Interference of two coherent laser beams

3. INSTRUMENTATION

The design of a laser interferometer for resist exposure is relatively simple, at least compared to state of the art mask e-beam lithography systems. In this section, we discuss the choice for the laser and optical path design.

3.1. Choice of Laser

A holographic setup to create 1, 2 and 3 dimensional gratings consists of respectively 2 or 3 or 4 beams from the same laser source coinciding at the same place under a given angle. The application and the spectral sensitivity of the substrate will be decisive for what type of laser will be suitable. The wavelength of the laser should match the sensitivity and absorption of the substrate. At the same time, the coherence-length should be long enough to overcome the optical path length difference. Pulse lasers have a short coherence length in the range of their pulse length, whereas Continuous Wave (CW) lasers have a very long coherence-length. CW- laser have the additional advantage in that it is easy to control the exposure dose by changing only the exposure-time. Light will only interfere with their polarization vector in the same direction; therefore a polarized laser will give the best result.

Basically two instrumentation architectures are found for Laser Interference Lithography: the *Lloyd's Mirror Interferometer*, which is used for high resolution, and the *Dual Beam Interferometer*, which is used for large areas.

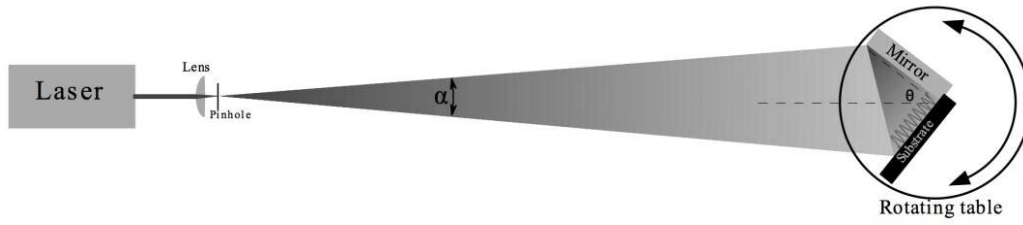


Figure 2. Lloyd's Mirror Interferometer

3.2. Lloyd's Mirror Interferometer

The simplest interference pattern to realize is a Bragg grating. This can be made with a so-called Lloyd's Mirror Interferometer that is composed of a laser with a long coherent Gaussian beam, a lens, a pinhole and a mirror. The mirror is placed perpendicular to the exposed surface (substrate) to create the second beam (see figure 2). If the substrate and mirror are placed on a rotating table the period of the Bragg grating can be easily and accurately changed. The lens and the pinhole are placed into the beam path to create a diverging beam. The laser beam should be s-polarized: the reflected and direct beams must have their polarization vector in the same direction to have optimal interference.

The beam centre is aligned at the intersection of the mirror and the substrate. The Gaussian beam should be symmetrically aligned over the substrate and mirror to have intensity I_1 equal to intensity I_2 .

At the intersection of mirror and substrate the angle θ_1 and angle θ_2 are equal. Away from the mirror the period will have an error because angle θ_1 and angle θ_2 are not equal. The angle θ_1 and angle θ_2 will change in relation to the diverging beam angle α .

$$\alpha = |\theta_1 - \theta_2| \quad \text{Equation 3.}$$

We can calculate this error by using a sine-rule and rewriting equation 2 to:

$$\Lambda = \frac{\lambda}{2 \cdot \sin\left(\frac{\theta_1 + \theta_2}{2}\right) \cdot \cos\left(\frac{\theta_1 - \theta_2}{2}\right)} \quad \text{Equation 4.}$$

The period Λ will be:

$$\Lambda = \frac{\lambda}{2 \cdot \sin(\theta)} \quad \text{Equation 4.}$$

where θ is the angle at the intersection of mirror and substrate and the error is

$$Error = 100 \cdot \left(1 - \frac{1}{\cos(\alpha/2)}\right)\% \quad \text{Equation 5.}$$

This error can be brought to zero by using a hyperbolic concave mirror to create a parallel beam where $\alpha = 0^\circ$.

The Lloyd's Mirror Interferometer is considered to be a "one beam interferometer". Since the mirror close to the substrate creates the second beam, only optical path differences between the mirror and substrate give rise to a disturbed interference pattern.



Figure 3. The Lloyd's Mirror interferometer on a vibration controlled table with air shield in the authors laboratory

To avoid optical path differences, airflow over the mirror and substrate should be minimized. Additional disturbance of the interference pattern due to vibrations can be reduced by placing the complete setup on a vibration-isolated table or on a very solid floor (Figure 3). Of course, the rotation table should be drift free during exposure.

The exposure area EA of the Lloyd's Mirror Interferometer is limited by size of the mirror M_x , M_y and the rotation angle θ :

$$EA = M_x \cdot M_y \cdot \tan(\theta). \quad \text{Equation 6.}$$

Since optically flat, big mirrors are expensive and difficult to handle, the exposure area is usually limited to a few square cm. Moreover, dust particles on the mirror will disturb the interference pattern. The mirror should have a perfect smooth surface with no tiny holes in the reflecting surface, so dielectric mirrors are to be preferred.

3.3. Dual Beam Interferometer

If a larger area is to be exposed a Dual Beam Interferometer setup is required. In a dual beam setup the laser beam is split into two beams. See figure 4. The two beams are expanded and filtered by a pinhole and both have to be aligned to the substrate. Their intensity and Gaussian profile should be the same and overlap at the substrate and their optical path length difference should be within the coherence length of the laser.

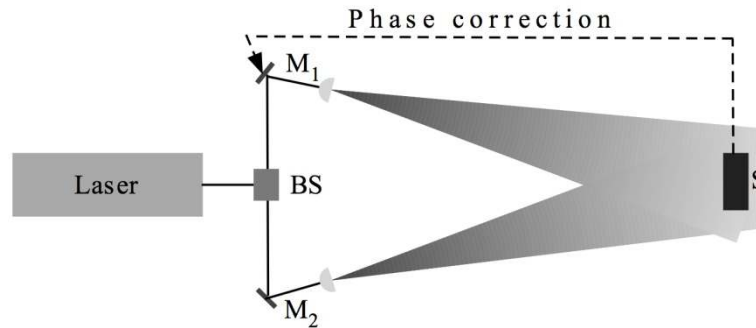


Figure 4. Dual Beam interferometer with beam-splitter BS and mirrors M1 and M2

The two beams in the Dual Beam interferometer have different optical paths. This difference makes the dual beam setup more sensitive to airflow. This airflow will give a phase difference between the two beams and the interference pattern will fluctuate. A phase-correction system is needed to compensate any change in phase due to this airflow. The phase difference should be measured close to the substrate. The airflow will also change the wave front. The wave front cannot be corrected and therefore it is recommended to use a cover shield to minimize any possible airflow (as in figure 3). Despite the cover shield, still very slow and small airflows will remain so a phase-correction system cannot be omitted. The dual beam interferometer needs more time to build and maintain. If you want to change the grating period Λ the setup has to be rebuilt and re-aligned. For 2D structures the substrate has to be placed on a rotating table itself and for 3D structures a more complex setup with more laser beams has to be made.

3.4. Requirements on Beam Size and Shape

The laser beam has a Gaussian intensity, which will give rise to a variation in exposure dose over the substrate. By expanding the laser beam to a size of 5 times the exposed area this variation will be reduced to 10%. The radius of a diverging Gaussian beam $W(z)$ at a large distance z can be calculated with:

$$W(z) = \frac{\lambda \cdot z}{\pi \cdot W_0} \quad \text{Equation 7.}$$

where W_0 is the radius of the beam at focus point and λ is the wavelength of the laser.

To steer the beam from the laser to the substrate at the right position highly reflecting mirrors are used. Due to impurities in the optical path, like dust on the steering-mirrors and laser-output, the wave front of the Gaussian beam will be disturbed. This wave front can be corrected by using an optical filter consisting of a lens and a pinhole. The diameter of the pinhole D_p is given by

$$D_p = \frac{4 \cdot \lambda \cdot f}{\pi \cdot w_b} \quad \text{Equation 8.}$$

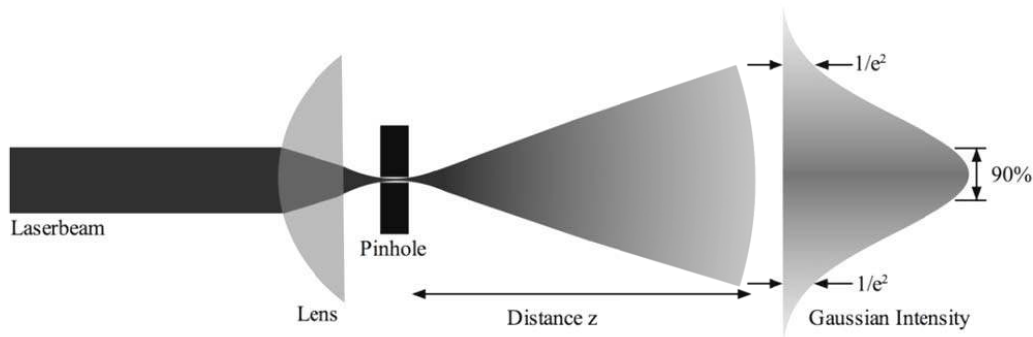


Figure 5. Focus in pin hole

where w_b is the radius of the laser beam and f is the focal length of the focusing lens. The energy of the laser beam is very high at focus. Standard pinholes will melt or at least get damaged by this high energy. Commercial available pinholes for high-energy application can resist energies up to 70MWatt/cm^2 . When focusing a laser however, the centre of the Gaussian beam is overriding this value easily. The alignment of the pinhole should always be done with low energy, but most lasers will change their beam path when set to lower energy, which severely complicates the alignment procedure.

Another problem is that these pinholes are more like a pipe instead of just a hole. (A $5\mu\text{m}$ high-energy pinhole has for instance a thickness of $15\mu\text{m}$.) At the focal point, the laser should fit into this pin-pipe instead of just a pin-hole (see figure 5). The width of the focused beam at the entrance of the pipe can be calculated from:

$$w(z) = w_0 \left[1 + \left(\frac{\lambda \cdot z}{\pi \cdot w_0^2} \right)^2 \right]^{1/2} \quad \text{Equation 9.}$$

Lens aberration will defocus the spot and filtering might become impossible, therefore a well-corrected microscope lens should be used.

The above consideration can be illustrated by the design calculations for our setup. To expose a 10 cm substrate with a Lloyd's Mirror Interferometer we use a 266 nm laser combined with a UV corrected microscope lens with a focus $f=11.53\text{ mm}$. The high-energy pinhole has a diameter D_p of $5\text{ }\mu\text{m}$ and a thickness of $15\text{ }\mu\text{m}$. To get the beam through the

pinhole with maximum energy and optimum beam shape we need to expand the beam to a radius w_d of 1.5 mm to achieve a w_0 of 0.55 μm . The beam diameter at the entrance of the pin-pipe will be 4.5 μm . To achieve a maximum intensity variation of 10% over a 10 cm wide substrate and mirror at $\theta=45^\circ$ the laser beam should be expanded to a size of $5 \times 10 \text{ cm} \times \sqrt{2} = 71 \text{ cm}$. This means that the substrate has to be placed at $z=460 \text{ cm}$ away from the pinhole. At $z=460 \text{ cm}$ the effective diverging beam angle α is $\text{atan}(14/460) = 1.75^\circ$. The maximum error in period Λ at $\theta=45^\circ$ will be not more than 0.01%

4. PHOTO-RESIST EXPOSURE

The intensity pattern in the diffraction grating is transferred to a photoresist layer. Since the angle of incidence of the light, as well as the wavelength, deviate from main-stream lithography, selecting the type of photoresist and the correct thickness is far from trivial. By using multiple exposures, more complex patterns than gratings can be realized.

4.1. Reflections and Standing Waves

The interference pattern created by the direct beam and the beam reflected from the mirror in the Lloyd setup is shown in figure 6a. A second interference pattern, caused by surface reflection is shown in figure 6b, and causes undesired standing waves in the vertical direction. This is especially a problem for highly reflecting layers such as silicon or metals.

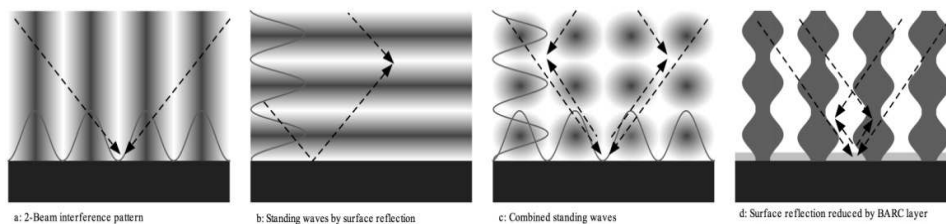


Figure 6. Reflection at surface

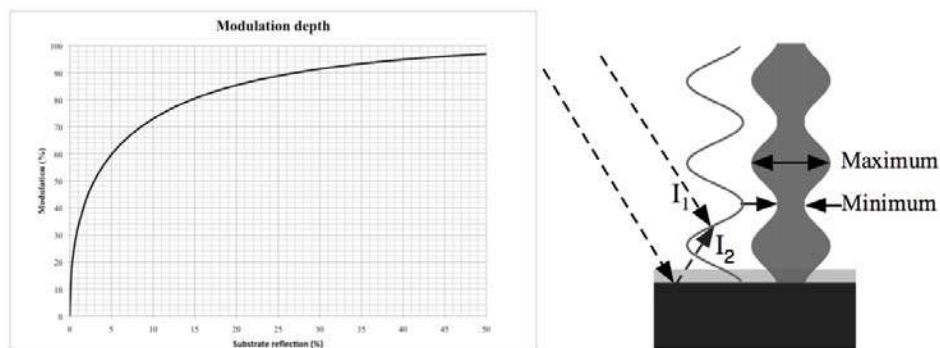


Figure 7. Modulation depth by interference between reflected and direct beam

The period of this vertical standing wave pattern is $\Lambda = \lambda / (n \cdot 2 \cos(a \sin(\sin \theta / n)))$ where n is the refractive index of the material. The reflectivity of the substrate is depending on the material property n and k and the angle θ and can be calculated with ellipsometry software.

The intensity profile or modulation of standing waves can be calculated from eq.1, where I_1 and I_2 are not equal. The modulation depth M is:

$$M = \frac{4 \cdot \sqrt{I_1 \cdot I_2}}{I_1 + I_2 + 2 \cdot \sqrt{I_1 \cdot I_2}} \cdot 100\% \quad \text{Equation 10.}$$

where I_1 is the intensity of direct beam and I_2 is the intensity of the beam reflected by the substrates. See figure 7.

A standing wave like this exists of knots and bellies. The knot is always at or close to the high reflecting surface, so there is no or little light close to the reflecting surface.

A high modulation depth might lace up the photoresist too much at the reflecting interface and the resist pattern will fall over. Silicon substrates reflect over 60% at an angle $\theta = 0^\circ$ and even more at larger angles. To reduce these reflections we can add an extra layer between the photoresist and the high reflective substrate: a so-called Bottom Anti Reflection Coating (BARC). To prevent the light from bouncing inside the photoresist layer a second anti reflection layer can be added on top of the photoresist. This Top Anti Reflection Coating (TARC) acts on the same principle as the BARC.

For optimal control of the standing waves both anti-reflection-coatings should be applied. How the antireflection layer works is explained in the next paragraph.

4.2. Anti Reflection Coating

To prevent reflection an extra layer can be added between the substrate and the photoresist. This layer should absorb the light and/or reflect it with a phase-shift π . At any transition of materials with different refractive index n light will reflect in relation to Fresnel's Law:

$$r = \left(\frac{n_1 - n_2}{n_1 + n_2} \right)^2 \quad \text{Equation 11.}$$

Figure 8 shows the antireflection layer with refractive index n_2 on a substrate with refractive index n_3 in an environment with refractive index n_1 .

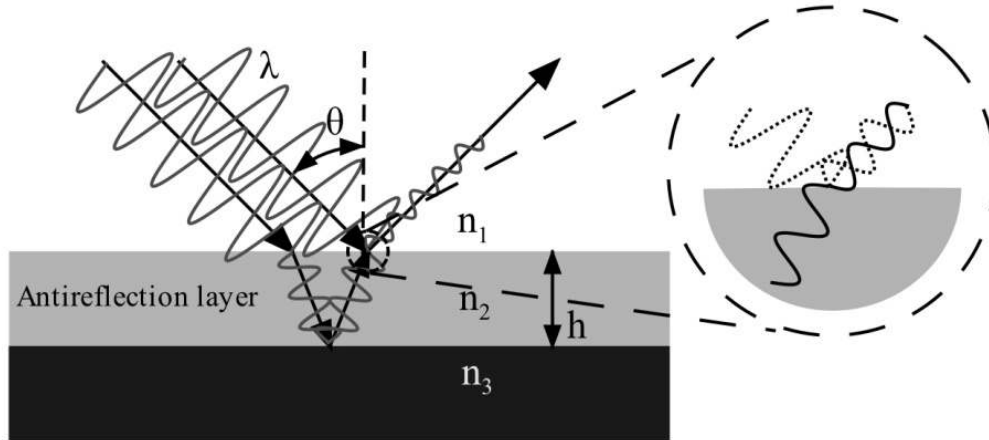


Figure 8. Reflection at an antireflection layer

The optical path length in the antireflection layer will give a phase shift ϕ . The phase shift ϕ is depending on the angle of incident θ , the refractive index difference between n_1 and n_2 , the thickness of the antireflection layer h and the laser-wavelength λ :

$$\phi = \frac{2 \cdot h \cdot n_2}{\lambda \cdot \cos \left[a \sin \left(\frac{n_1}{n_2} \cdot \sin \theta \right) \right]} \quad \text{Equation 12.}$$

If the intensity of the reflection from transition n_1 - n_2 is equal to the intensity of the reflection from transition n_2 - n_3 and the phase difference ϕ is an odd number of π : the total reflection is canceled out.

Commercially available BARC's uses a combination of absorption and phase-shift. This combination makes these BARC's less critical to the substrate surface parameters n and k . BARC in UV-Lithography is made for 3 wavelengths: the 365 nm wavelength (i-line), 248 nm (KrF) and 193 nm (ArF). These BARC's are made for direct use on silicon or metal surfaces. If the laser has another wavelength, the BARC might not work properly. For example, the Brewer Science DUV52D is optimized for 248 nm and has a minimum reflection around 60 nm thickness. The setup in the authors' lab operates at 266 nm, where the minimum reflection is at 170 nm. See figure 9. The reason for this is that the refractive parameters of DUV52D at 248 nm are $n = 1.9$ and $k = 0.43$. The refractive parameters at 266 nm however are $n = 2.07$ and $k = 0.23$. The imaginary refractive index k is much lower at 266 nm and therefore the absorption is less and the BARC-layer is less efficient.

Figure 10 shows the effect of BARC-layer thickness from 5, 10, 20, 30, 40 and 50nm in positive photoresist on a high-reflective silicon substrate with the same exposure dose. From a series of experiments like this, the optimum BARC layer thickness can be selected. In positive-resist the exposed resist is resolved in the developer. When the BARC-layer thickness increases the reflection becomes less and the structures become thicker at the bottom waist. From calculations we expected that 40nm of BARC-layer thickness should give the optimum effect. The effective phase shift would be π . Unfortunately there is a knot at the

interface between photoresist and the BARC-layer and due to the threshold there is a residue of photoresist, as can be seen in figure 10. The BARC Layer is hard to remove without damaging the structure. Therefore a lower thickness of BARC-Layer should be applied.

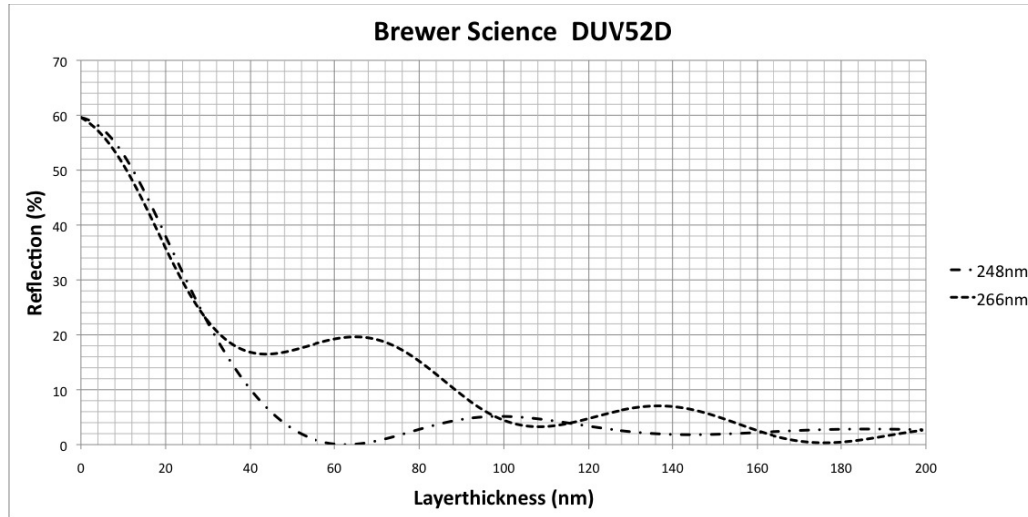


Figure 9. Reflection at the BARC Layer at 248 nm and 266 nm

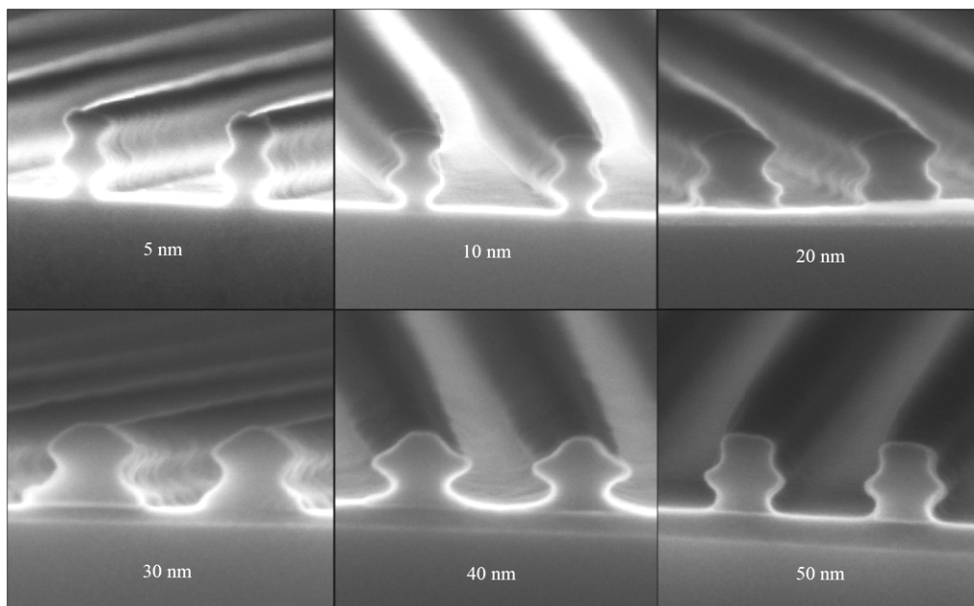


Figure 10. Positive photoresist with BARC layer thickness variation from 5 to 50nm

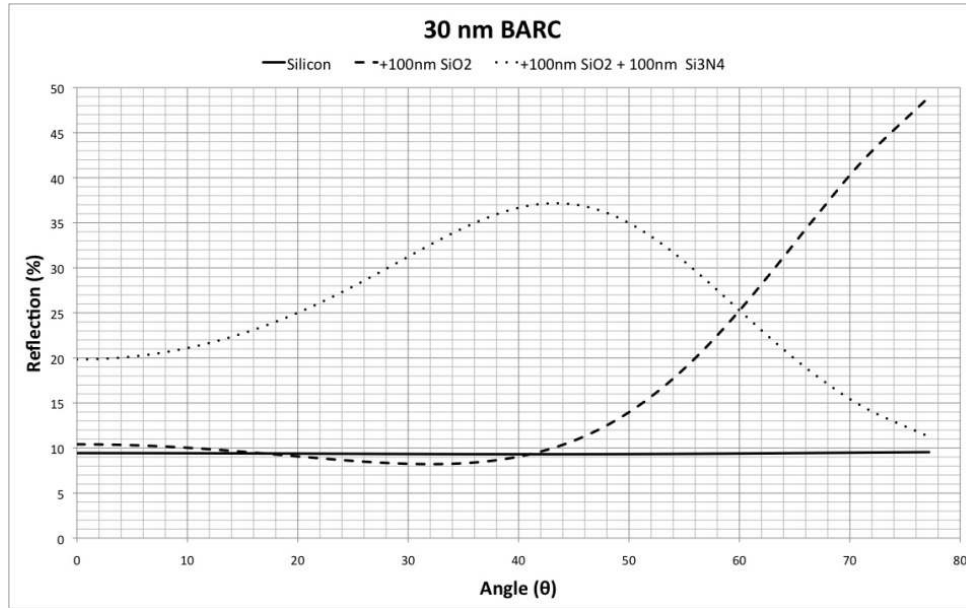


Figure 11a. 30nm BARC at different layers

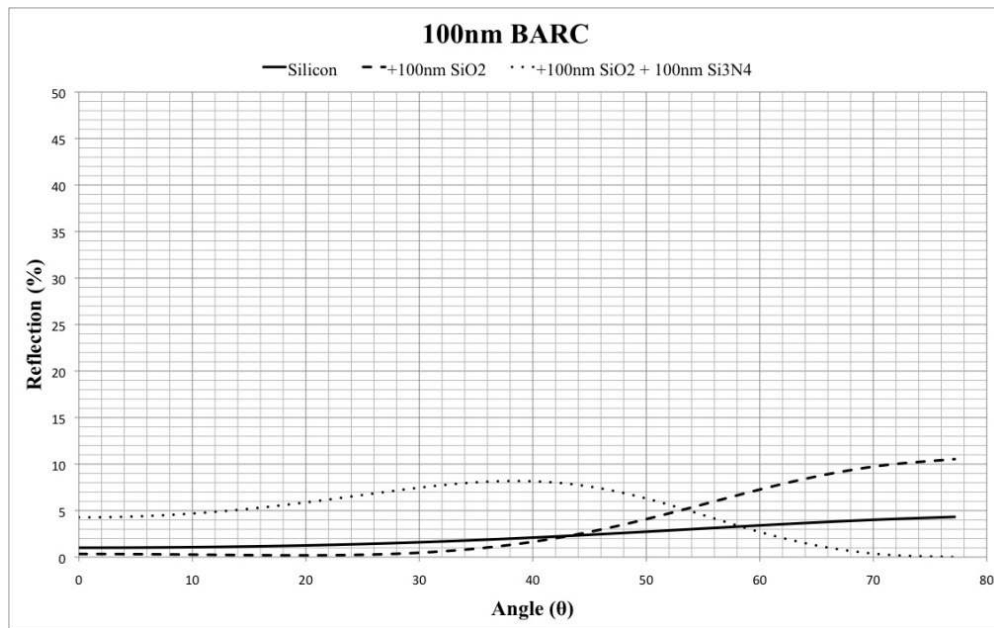


Figure 11b. 100nm BARC at different layers

When using optically transparent (thin) layers the results of the calculations change, as well as using different incidence angles, as is shown in figures 11a and b. In experimental environments the parameters of the layers are not exactly known or even reproducible. Optical calculations are therefore a good starting point, but the BARC-layer thickness often needs to be optimized by experiment.

4.3. Selection of Photoresist

For a line pattern like the Bragg grating it is not important whether a negative or a positive resist is used. Photosensitive layers in general are defined by their spectral sensitivity, photosensitivity, contrast and threshold. The minimum intensity to activate the photoresist is called the threshold. The spectral sensitivity should match the laser wavelength. Photosensitivity is important in industrial environments to keep the processing time low. Contrast and threshold are effective on the modulation depth of the resist shape. High-contrast photoresist will amplify the modulation depth of the resist shape. The threshold will amplify the modulation depth only in negative resist and reduces the modulation depth in positive resist. However due to the intensity-knot at the surface there will be some residues of unresolved positive photoresist (see figure 10b, 11d and 11e). Negative photoresist will have no residues of unresolved resist left at the surface but might not have enough adhesion to the substrate (see figure 10a).

If the BARC-Layer is tuned to the correct thickness like in figure 13a the shape of the structure will always have some imperfections due to roughness, particles in the photoresist or side effects like bridging in figure 13b.

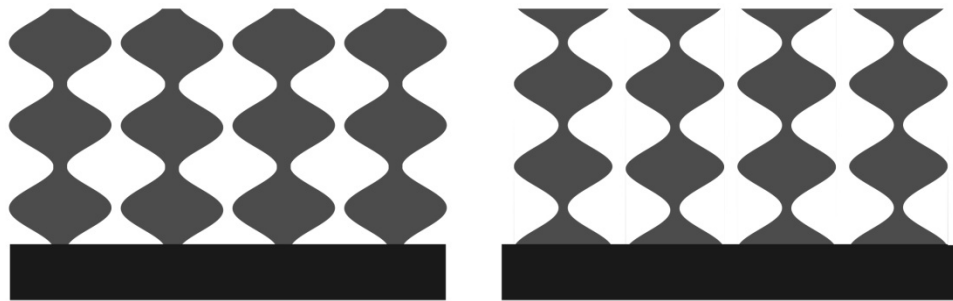


Figure 12a. Negative resist pattern with reflection (b). Positive resist pattern with reflection

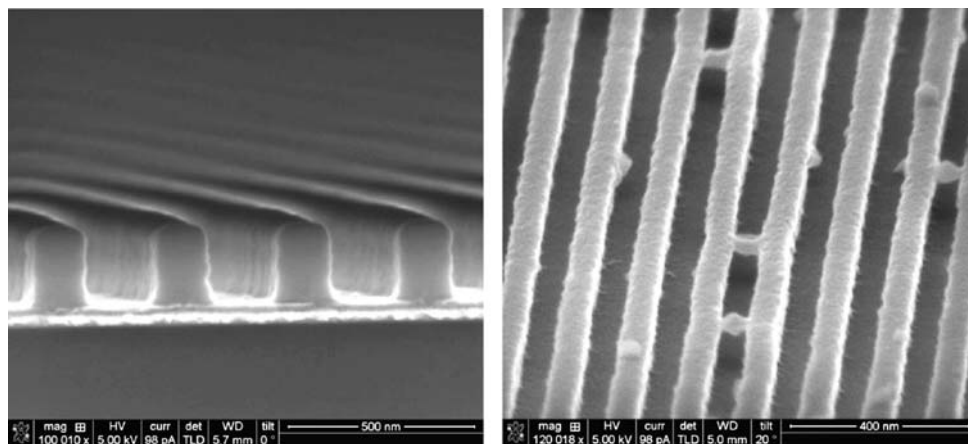


Figure 13a. Good BARC-Layer Thickness (b). Bridging effect in negative photoresist

4.4. Multi Exposure

In a more complex pattern more than one exposure is needed. The desired structure defines the choice between negative or positive resist. Expanding the Lloyd's Mirror Interferometer with a rotating substrate holder opens a whole new world of patterns. Rotating the substrate over an angle β and expose the substrate a second time creates new patterns like isolated lines, cubic and hexagonal structures of pillars and holes.

The substrate can be exposed many times. Changing the angle β between 2 exposures is shown in figure 14b.

Rotating the sample 90 degrees between two exposures with the same period are shown in figure 15. The pillars are made on a cobalt layer and the holes are made on a SiO_2 layer. The BARC-Layer is optimized to have a clean substrate, not a minimum reflection.

Rotating the substrate 60° results in hexagonal structures. Unfortunately the shape of the holes of pillars will become elliptical. To make circular holes or pillars in a hexagonal structure the Lloyd's Mirror Interferometer should have two mirrors at 120° to each other[5]. All combinations of rotation angle and changing the period are possible until all the photoresist is exposed. See Figure 16.

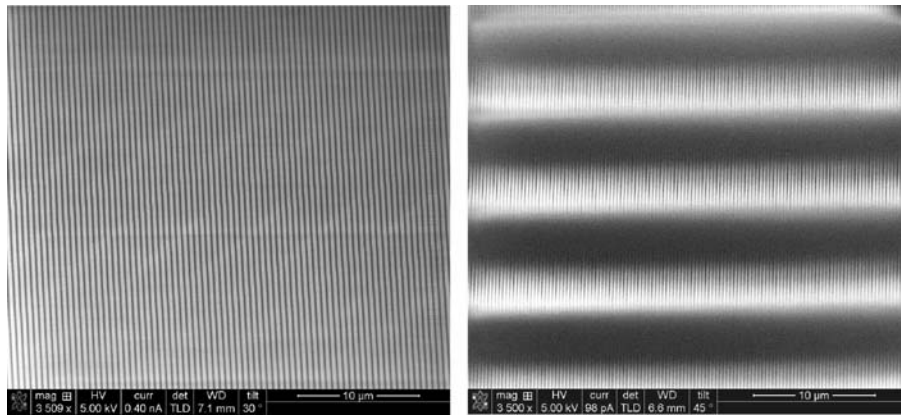


Figure 14a. Single exposure (b). Double exposure with 1° rotation

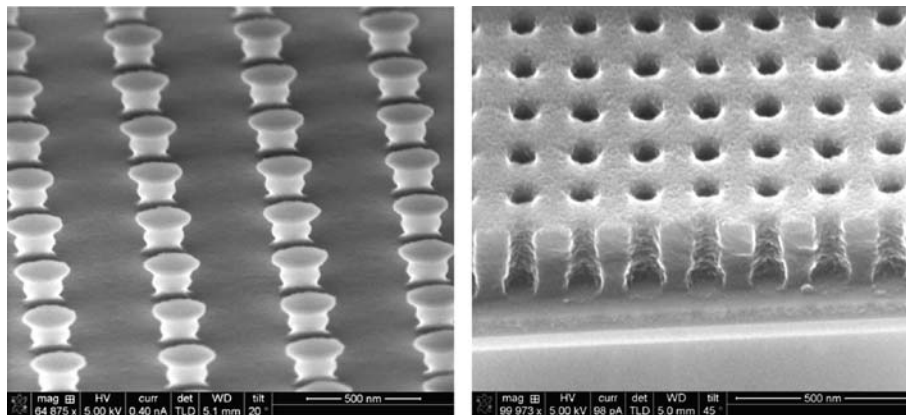


Figure 15. Double exposure with 90° rotation with positive and negative resist

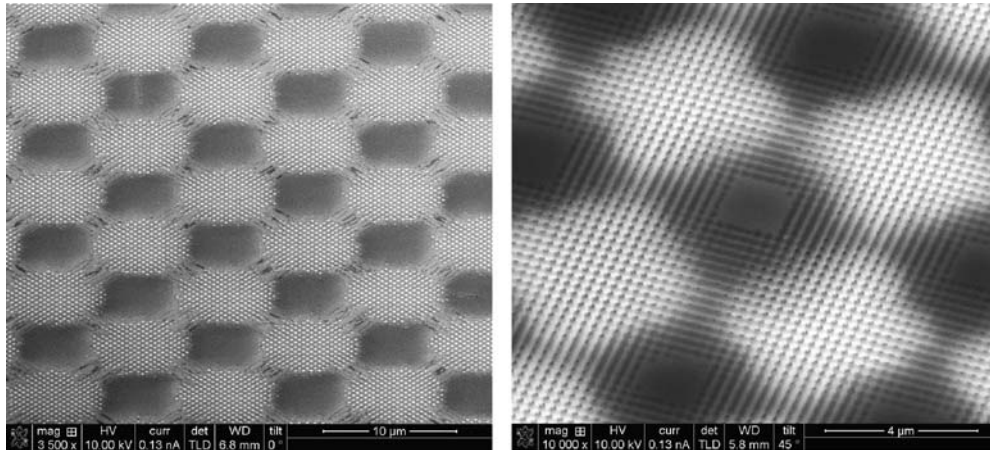


Figure 16. Quadruple exposures of two superimposed periods at 60° and 90° rotation in positive resist.

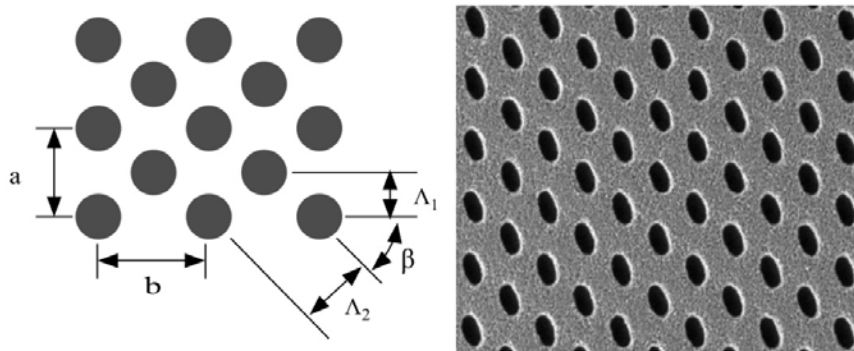


Figure 17. Face centered orthorhombic lattice

It is easy to make a crystal-like structure with different lattices at angles other than 60° or 90° on a Lloyd's Mirror Interferometer with a rotating substrate holder placed on a rotation table. Expose the substrate at an angle θ_1 for period Λ_1 , rotate the in a substrate holder over a defined angle and expose the substrate again at an angle θ_2 for period Λ_2 . To create a face centered orthorhombic lattice where $b = \sqrt{2}a$ for example, we need a double exposure with period $\Lambda_2 = 1.15 \times \Lambda_1$ and $\beta = 54.7^\circ$. To make such a pattern on another kind of interferometer will take much more time.

CONCLUSION

Laser Interference Lithography is a flexible tool for lithography to create periodic patterns in photoresist. The setup is relatively simple, and by using the Lloyd's Mirror configuration, periodicities and pattern directions can be easily changed. It is advisable to use continuing wave lasers. Due to the high intensities used, special care must be taken when selecting pinholes for optical filtering. Since the angle of incidence and wavelength of the

laser are different from mainstream lithography lines, extra effort has to be put into optimizing anti-reflection coatings. By using multiple exposures, under varying angles, a wealth of periodic patterns can be realized which can find their way into many different applications.

REFERENCES

- [1] *Optics*, Hecht, Zajac, 1984.
- [2] *Fundamentals of Photonics*, B.E.A. Saleh, M.C. Teich, 1991.
- [3] *The CVI Melles Griot Technical Guide*, 2009.
- [4] Langenbeck, PH. *Applied Optics*, 1967, Vol.6, No 10.
- [5] Johannus de Boor, *Optics Letters*, 2009, Vol34, No 12
- [6] Haast, MAM. *Journal of Magnetism and Magnetic materials*, 1999, Vol 193, 1-3.
- [7] Van Rijn, *Journal of micromechanics and microengineering*, 1999, Vol 9, No 2.
- [8] Vogelaar, L. *Advantage Materials*, 2001, Vol 13, 20.